ISSN 0869-5911, Petrology, 2006, Vol. 14, No. 5, pp. 477–491. © Pleiades Publishing, Inc., 2006.
Original Russian Text © N.L. Dobretsov, A.A. Kirdyashkin, A.G. Kirdyashkin, I.N. Gladkov, N.V. Surkov, 2006, published in Petrologiya, 2006, Vol. 14, No. 5, pp. 508–523.

Parameters of Hotspots and Thermochemical Plumes during Their Ascent and Eruption

N. L. Dobretsov, A. A. Kirdyashkin, A. G. Kirdyashkin, I. N. Gladkov, and N. V. Surkov

Institute of Geology and Mineralogy, Siberian Division, Russian Academy of Sciences, pr. Akademika Koptyuga 3, Novosibirsk, 630090 Russia

e-mail: dobr@uiggm.nsc.ru

Received February 27, 2006

Abstract—Thermochemical plumes develop at the core–mantle boundary in the presence of a heat flow from the outer core and at local chemical doping that decreases the melting temperature near the bottom of the lower mantle (this dope triggers the melting of the mantle material and the ascent of the plume). The paper presents evaluations for the heat power of the Hawaiian and Iceland plumes and the results of the experimental modeling of a thermochemical plume. The diameter of a plume conduit was determined to remain virtually unchanging in the course of plume ascent. When the top of a plume reaches a "refractory" layer, whose melting temperature is higher than the melt temperature in the plume conduit, a mushroom-shaped head of the plume develops beneath the bottom of this layer. The analysis of geological and geophysical data and the results of experimental modeling are used to develop a thermal physical model for a thermochemical plume. The balance relations for the mass and thermal energy and systematic tendencies in the heat and mass transfer during free convection were utilized to derive a system of equations for the heat and mass transfer of a thermochemical plume. Parameters were determined for a thermochemical plume ascending from the core–mantle boundary. Geodynamic processes are considered that occur during the ascent of a plume before it reaches the surface. The effect of the *P–T* conditions on the shape and size of a plume roof is analyzed, and a model is proposed for mass transfer between a thermochemical plume and the lithosphere, when the plume reaches the bottom of a "refractory" layer in the lithosphere.

DOI: 10.1134/S0869591106050043

INTRODUCTION

This publication presents the principal results obtained in the course of our long-term research (Dobretsov, 1980, 1997; Dobretsov et al., 1993, 2001, 2003, 2005, 2006; Dobretsov and Kirdyashkin, 2000; Kirdyashkin and Gladkov, 1994; Kirdyashkin et al., 2004, 2005) of the source of mantle plumes discernible at the surface in the form of hotspots, their origin regions, thermal power, and the principal parameters of currently active plumes, such as the Hawaiian and Iceland plumes. It was established that thermochemical plumes originate from the core–mantle boundary. The experimental modeling and theoretical analysis of the heat and mass transfer made it possible to obtain the principal parameters of thermochemical plumes during their ascent to the surface and eruption.

The authors were pleased to accept the invitation to contribute to the issue of *Petrology* devoted to the 80th birthday of Acad. V.A. Zharikov, one of Russia's leading researchers in the field of physicochemical geology. His studies of magma generation in the mantle (Zharikov, 1976; *Experimental Problems…*, 1994) have stimulated extensive experimental and theoretical investigations into related problems.

THEORETICAL CONSIDERATIONS

The analysis of heat transfer in the outer core (Dobretsov et al., 2001, 2003) indicates that the superadiabatic temperature difference in the outer core during heat–gravitational convection does not exceed 0.1°C at a heat flow at the core–mantle boundary q = 0.06–0.6 W/m^2. The reason for this insignificant temperature difference is the high thermal conductivity of the outer core (Manga and Jeanloz, 1996) and its low kinematic viscosity $\nu = 1–10^2$ m^2/s (Dobretsov et al., 2001). The low temperature differences in the outer core at the core–mantle boundary preclude purely thermal sources, which cause the origin of plumes with a thermal power $N \sim 10^8$ kW, as is typical of modern plumes (see below).

At the same time, it is reasonable to expect that local flows of volatiles (H_2, CH_4, and others) characterized by a high solubility in a liquid Fe melt (+Ni) can occur at the core–mantle boundary (Dobretsov et al., 2003; Kirdyashkin et al., 2004), are focused within the central portion of funnel-shaped vortexes (Dobretsov and Kirdyashkin, 2000), and, as a consequence, give rise to thermochemical plumes.

A thermochemical plume can be formed at the boundary of two layers in the presence of a heat flow from the lower layer and at local chemical doping that

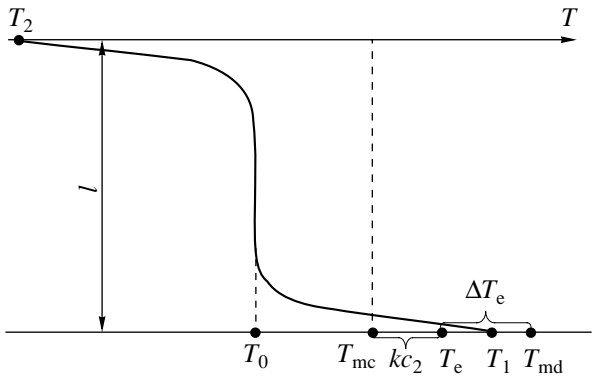

Fig. 1. Temperatures at which thermochemical plumes can be formed.

decreases the melting temperature near the bottom of the upper layer. Within a thermal boundary layer, a decrease in the melting temperature of the upper layer bottom triggers its melting and the ascent of the plume.

The problem of the thermochemical nature of mantle plumes (Tackley, 2002) was discussed at an international conference devoted to superplumes that was held in 2002 in Tokyo. Theoretical considerations generally suggest that the presence of aqueous components should significantly affect the origin of plumes at the core–mantle boundary (Saxena, 2002). We have evaluated some parameters of thermal plumes (Dobretsov et al., 1993) from the results of the theoretical and experimental modeling of free convective heat transfer and the convection structure of plumes. This publication is devoted to the condition under which thermochemical plumes are formed and their principal characteristics.

If there is a local source of a dope decreasing the melting point, a thermochemical plume can form.

The rate of melting in the plume conduit should depend on the relations between the plume sole temperature T_1, the average temperature over the thickness of the layer–massif T_0, and the melting temperature of the massif in the presence of a chemical dope T_{mc}. A thermochemical plume can be formed where a chemical dope is concentrated that suppresses the melting temperature to the value of T_{mc} (Fig. 1), under the condition $T_0 < T_{mc} < T_1$. In the process of melting, the heat coming from the plume base is spent on heating to the melting temperature, on melting itself, and sinks into the ambient massif, because $T_0 < T_{mc}$. The heat flow from the lower boundary to the plume is the higher, the higher the temperature difference $T_1 - T_{mc}$. The heat flow from the conduit to the ambient massif is the lower, the lower the temperature difference $\Delta T_0 = T_{mc} - T_0$.

If the addition of the chemical dope creates an eutectic with a temperature T_e (Fig. 1), then $T_{mc} = T_{md} - T_e - kc_2 = \Delta T_e - kc_2$, where T_{md} is the melting temperature of "dry" massif (without dope), $\Delta T_e = T_{md} - T_e$, the coefficient k is in °C per 1% of the dope, and c_2 is the concentration of the dope at the melt–massif boundary (at the boundaries of the plume conduit). If $\Delta T_e = 0$, $T_{mc} = T_{md} - kc_2$. In the absence of a dope decreasing the melting temperature, $k = 0$, and then $T_{mc} = T_e$. Since $T_{mc} = T_{md} - kc_2$, $T_1 - T_{mc} = kc_2 - (T_{md} - T_1)$. The melting of mantle material can occur in the vicinity of the core–mantle boundary if the difference $(T_1 - T_{mc})$ is positive, i.e., the condition $kc_2 > T_{md} - T_1$ is met, and hence,

$$c_2 > (T_{md} - T_1)/k. \quad (1)$$

The melting rate of a thermochemical plume should depend on the parameters that control the supply of the chemical dope, first of all, on the diffusion coefficient D and the concentration of the chemical dope in the plume conduit. Depending on the heat flow from the bottom, the conduit can be melted throughout the whole thickness of layer l or to a height $L < l$. In the latter instance, the quantity of heat transferred from below to the plume conduit of height L is equal to the quantity of heat coming from the conduit to the ambient massif. The height L is limiting for this quantity of heat transferred from below.

The dope suppressing the melting temperature is thought to be provided by reactions between Fe-bearing lower-mantle minerals (perovskite and magnesiowuestite) with hydrogen and/or methane that are released at the core–mantle boundary (Dobretsov et al., 2003; Kirdyashkin et al., 2004).

EVALUATION OF THE THERMAL POWER OF THERMOCHEMICAL PLUMES

The thermal power of a plume can be calculated from the volume of the magma that ascended and erupted above the lower topographic level of a given plume. This volume can, in turn, be assessed from the residual topography of the plume trace above the lower topographic level in the vicinity of the plume. The ascent and eruption of magma occur mostly because of the thermal expansion of the mantle material heated by the plume source. Knowing the time needed for the elevation above the topographic level, one can calculate the volume of material that was ascending per time unit or, in other words, the specific volumetric flux ΔV_f (m^3/s), which can be used to calculate the specific mass flux

$$\Delta G = \rho_f \Delta V_f, \quad (2)$$

where ρ_f is the density of the uplifted rocks.

The specific mass flux can be determined from the relation

$$\Delta G = G\beta\Delta T, \quad (3)$$

where G is the mass of the mantle material heated by the plume source per time unit, ΔT is the average temperature increase of the heated material of mass G relative to the temperature of the ambient massifs, and β is the coefficient of thermal volumetric expansion. The

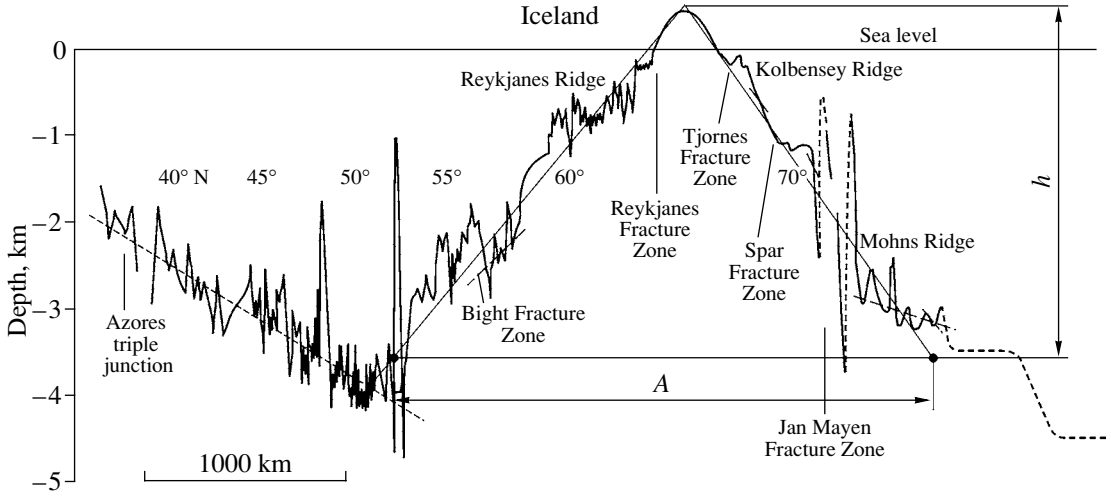

Fig. 2. Topographic profile along the crest of the Mid-Atlantic Ridge (after Seifert, 1991; Vogt, 1976).

mass of the mantle material G heated per time unit can be found from Eq. (3):

$$G = \Delta G/\beta\Delta T. \quad (4)$$

The thermal power of the plume source is derived from the relation

$$N = GC\Delta T + B\Delta G, \quad (5)$$

where B is the melting heat of the mantle material, and C is the heat capacity of this material. The first summand in (5) involves the heat spent on the heating of the mantle material, and the second summand is the melting heat of the erupted magma. Substituting (4) into (5), we obtain

$$N = \Delta G\left(\frac{C}{\beta} + B\right). \quad (6)$$

Relation (6) involves all heat of the source: the heat transferred from the plume conduit to the lower and upper mantle and the heat spent on melting. The thermal power of a plume can be calculated from actual data on the mass of the uplifted material and physical characteristics (C, β, and B). Note that the value of B is one order of magnitude smaller than the value of C/β and, hence, can be neglected.

This technique can be applied to determine the thermal power of plumes beneath oceanic plates (for example, the Hawaiian and Bouvet plumes) and continental plate, as well as the power of plumes at the axes of mid-oceanic ridges (for example, the Iceland plume) (Dobretsov et al., 2005).

Now we can assess the thermal power of the Iceland plume at the axis of the Mid-Atlantic Ridge. The axial zone of this ridge is characterized by the ascent of plume magma and its intrusions and eruptions and by the subsequent moving apart of the crystalline rocks on both sides of the ridge axis with a velocity (spreading half-rate) u = 1 cm/year = 3.17×10^{-10} m/s (Rona, 1984). The thermal power of the Iceland plume can be evaluated from relation (6). The topographic profile of the Iceland plume along the MAR axis (Fig. 2; Seifert, 1991; Vogt, 1976) can be used to quantify the cross section of the erupted rocks elevated above the lower topographic level. As can be seen in Fig. 2, the flux of asthenospheric material heated above the plume spreads along the ridge axis for a distance A = 2700 km. According to data from (Ito and Lin, 1995), the value of A at u = 1 cm/year is equal to 2800 km. The height of the ridge h = 4.1 km. The cross section of the topographic profile along the ridge $S = Ah/2 = 5.54 \times 10^9$ m^2. The ascending volume flux $\Delta V_f = 2Su = 3.5$ m^3/s, and the mass flux $\Delta G = \rho_f \Delta V_f = 9.45 \times 10^3$ kg/s at $\rho_f = 2700$ kg/m^3. According to (6), the thermal power of the Iceland plume at $\beta = 3 \times 10^{-5}$°C^{-1} and C = 1.2 kJ/(kg °C) is $N = 3.78 \times 10^8$ kW.

The thermal power of the Hawaiian plume is evaluated as follows. Figure 3 displays the variations in the mass and volume fluxes with time for the Hawaiian hotspot during the passage of the Pacific plate above it (Vogt, 1979). The volume flux ΔV_f is determined from topographic profiles in the plane perpendicular to the Hawaiian volcanic chain, from the topographic elevation above the lower topographic level for the cross section in question near the volcanic chain. The modern specific heat flow of the Hawaiian hotspot is ΔV_f = 2.8 m^3/s, and, at $\rho_f = 2700$ kg/m^3, the specific mass flux $\Delta G = \rho_f \Delta V_f = 7560$ kg/s. At $\beta = 3 \times 10^{-5}$°C^{-1} and C = 1.2 kJ/(kg °C), (6) yields a thermal power $N = 3.0 \times 10^8$ kW.

The thermal-power scale in the right-hand side of Fig. 3 for the Hawaiian plume corresponds to the ascending mass flux and was calculated from (6). The actual modern value of ΔV_f can be calculated accurately enough, because the mantle material anomalously heated under the effect of the plume cools with time, so that the height of the elevation decreases. This can

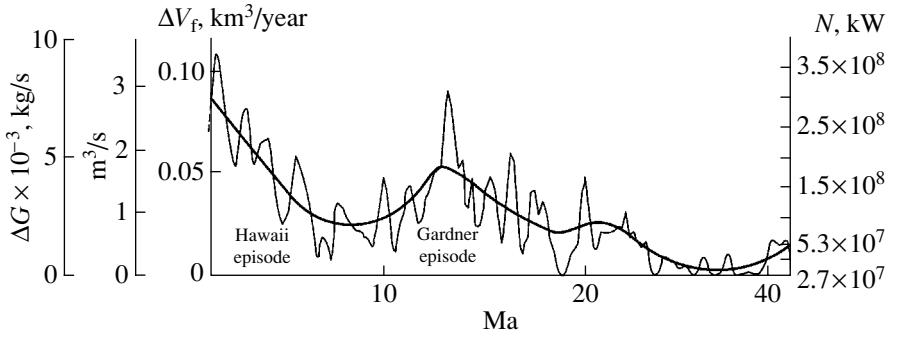

Fig. 3. Temporal variations in the specific mass flux ΔG and the volume ΔV_f of magmas erupted in relation to the Hawaiian plume (Vogt, 1979). The thermal power of the plume source N was calculated from relation (6) in compliance with the temporal variations in the ΔV_f and ΔG values.

account for the decrease in the average ΔV_f with time for the Hawaiian plume. As follows from Fig. 3, the averaged magma discharge decreases not monotonously but displays systematic periodical variations with time. The possible reason for the short-term variations in ΔV_f, with a period of ~1.8 m.y., is the periodical shifts in the conduit of the eruptions during the movement of the Pacific plate above the Hawaiian plume and/or the rotation of the plume with deviations from the vertical axis, which is commensurable with the diameter of the plume conduit (Dobretsov et al., 1993, 2001; Dobretsov and Kirdyashkin, 1998). The variations with a period close to 15 m.y. are correlated with the period of variation in the frequency of magnetic reversals and likely reflect fluctuations in the intensity of the plume itself at the core–mantle boundary (Dobretsov et al., 2001; Larson and Olson, 1991; Dobretsov and Kirdyashkin, 1998). The low-frequency variations in the specific volume flux and thermal power of the Hawaiian plume are correlated with three regional indexes of volcanism along the perimeter of the Pacific Ocean: the specific volumes of eruptions in the Southwest Pacific, Central America, and Central Oregon (Vogt, 1979).

Our analysis of the heat and mass transfer in the presence of a chemical dope that suppresses the melting temperature of the mantle material has demonstrated that a heat flow with a thermal power equal to 3.0×10^8 kW from the bottom of a thermochemical mantle plume 100 km in diameter is possible only at the thermophysical properties of the outer core. Because of this, the sources of thermochemical plumes of this thermal power can occur only at the core–mantle boundary. An important argument in support of the origin of plumes at the core–mantle boundary is the correlation between the intensity of mantle plume magmatism and the number of magnetic reversals, which are likely related to processes in the outer core (Dobretsov et al., 2001; Larson and Olson, 1991; Dobretsov and Kirdyashkin, 1998). The time needed for a single plume to reach the surface is comparable with an average inversion period and can vary from 0.5 to 5 m.y. (Dobretsov et al., 2001, 2005; Kirdyashkin et al., 2004).

EXPERIMENTAL MODELING

We modeled experimentally the derivation (via melting) of thermochemical and thermal plumes at the core–mantle boundary. Below we present a brief description of our model experiments and their principal results important in the context of this publication. The experimental set-up for the modeling of conditions under which a thermochemical plume is produced at the core–mantle boundary was a glass vessel (Fig. 4, *1*) 245 mm in diameter and 250 mm high with a cylinder (*3*) of quartz glass 93 mm in diameter and 200 mm high or a glass cylinder 128 mm in diameter and 120 mm high, which were mounted on a stand (*2*) 95 mm high. The cylinder was filled with molten paraffin (*4*), which then solidified. The glass vessel was filled with thermally-controlled water (*5*) to the upper boundary of the solid paraffin. The water temperature was varied in discrete experiments from 40 to 47°C. The level of water in the vessel was maintained at a specified constant height by the pump of the thermostat. In these experiments, the bottom of the solid cylindrical paraffin massif was in contact with the liquid, and the water column exerted a constant pressure on the plume base. Thus conditions were modeled corresponding to those of plume growth at the boundary of the highly viscous lower mantle and the much less viscous outer core. The cylindrical electric heater (*6*) 6 mm in diameter was in contact with the bottom of the paraffin massif at the wall of the cylinder filled with paraffin. The heater (source of thermal energy, *6*) and a capillary (*7*) for the introduction of the chemical dope (hexadecane) modeled conditions under which a thermal plume develops at the core–mantle boundary. The process of the development of a plume in paraffin was periodically videotaped through the glass walls of the vessel. In brief, the videotaped ascent of the plume through the paraffin massif was as follows.

The experiments were carried out in the following manner. A heater (*6*) was introduced into paraffin (melt-

ing point 52°C) at a height of ~10 mm. The power of the heater was not sufficient for melting the paraffin, so that a thermochemical plume could develop only if the paraffin was doped with hexadecane near the heater (the dope was introduced via capillary *7*). The design of the capillary allowed the experimentalist to introduce small portions of hexadecane into paraffin. The introduction of the dope (hexadecane, melting point 18.8°C) through the capillary decreased the melting temperature of the paraffin and initiated its melting and the ascent of the newly formed thermochemical plume (*8*). The temperature at the melt–solid paraffin boundary was measured at the top of the plume and was equal to 47–50°C, i.e., lower than the melting point of paraffin.

In the course of melting, the volume of molten paraffin increased due to the melting and an increase in the melt temperature relative to the colder solid paraffin, i.e., the volume of the melt eventually became greater than the volume of the solid paraffin. Because of this, the excess volume of the melt was outpoured near the bottom of the ascending plume and was accumulated at the water–paraffin boundary, which imitated the core–mantle boundary (and was videotaped in the course of our experiments). When the thermochemical plume developed, the melting temperature of the paraffin doped with hexadecane was lower than the temperature of the ambient water, and hence, the excess melt at the water–paraffin boundary (at the plume base) did not solidify.

When the top of the plume reached the upper boundary of the paraffin massif, molten paraffin outpoured from the plume conduit. The process of paraffin eruption differed in the modeled thermochemical and thermal plumes.

The eruption of the **thermochemical plume**, which developed after paraffin doping with hexadecane, occurred in two stages. As the plume broke through, it started to erupt the melt accumulated near the bottom of the cylindrical paraffin massif. After this, water ascended along the plume conduit from the plume base (i.e., from the paraffin–water interface) and squeezed upward a volume of melt equal to the volume of water that had ascended along the conduit. The height x_w to which water ascended along the conduit can be determined from the condition that the pressure of the water column of height H_w in the plume base $\rho_w g H_w$ (g is the gravitational acceleration) should be equal to the sum of the pressure exerted by the molten paraffin column $\rho_m g H_m$ (which has a height $H_m = H_w + x_p - x_w$) and the pressure of the water column in the conduit $\rho_w g x_w$ (Fig. 4): $\rho_w g H_w = \rho_m g\,(H_w + x_p - x_w) + \rho_w g x_w$. This equation leads to the relation

$$x_w = H_w - \frac{x_p \rho_m}{\rho_m - \rho_w}, \qquad (7)$$

where x_p is the elevation of the paraffin level above the water level in vessel (*1*) (Fig. 4), ρ_w is the density of water, and ρ_m is the density of the melt.

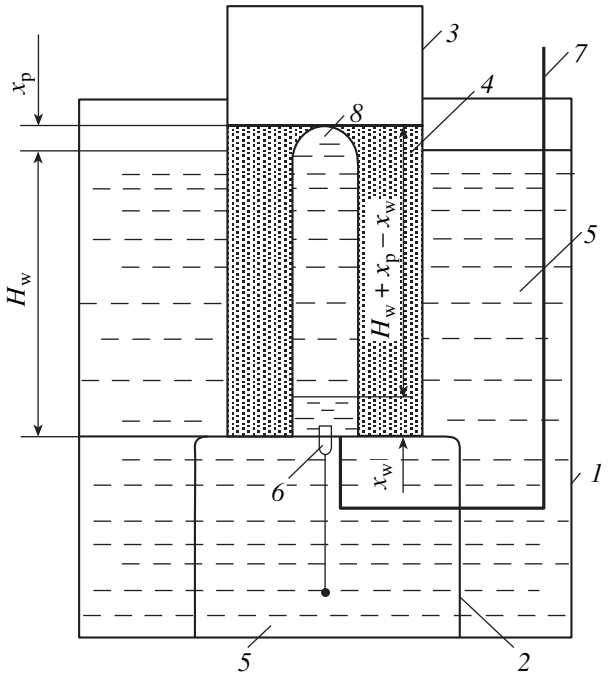

Fig. 4. Experimental set-up for the modeling of a thermochemical plume. (*1*) Glass vessel; (*2*) support of acrylic plastic; (*3*) transparent cylinder of quartz glass; (*4*) solid paraffin; (*5*) water; (*6*) electric heater; (*7*) capillary for introducing hexadecane; (*8*) plume. The scheme illustrates the situation when the paraffin melt is erupted because of the intrusion of water into the plume conduit to a high x_w.

Proceeding from this result, we can calculate the height to which the material of the outer core (which ascended from the core–mantle boundary) should be uplifted within the mantle plume conduit and then erupted to the surface. After the eruption of the plume at the surface, the lithostatic pressure at the core–mantle boundary ($\rho_0 g H$) is counterbalanced by the pressure of the melt column of height $H - x_{oc}$ in the plume conduit [$\rho_m g(H - x_{oc})$] and the pressure of the column of outer core material of height x_{oc} that has ascended in the plume conduit ($\rho_{oc} g x_{oc}$): $\rho_0 g H = \rho_m g(H - x_{oc}) + \rho_{oc} g x_{oc}$. From this relation, we can derive the height to which the outer core material should ascend in the mantle plume conduit

$$x_{oc} = H(\rho_0 - \rho_m)/(\rho_{oc} - \rho_m), \qquad (8)$$

where H is the distance from the core–mantle boundary to the surface, ρ_0 is the average density of the mantle, ρ_m is the average density of the melt in the plume conduit, and ρ_{oc} is the density of the outer core material. Considering that the difference between the densities $\rho_0 - \rho_m = \rho_0 \beta(T_m - T_0) = \rho_0 \beta \Delta T$ (where T_m is the melt temperature in the plume conduit, T_0 is the temperature of the ambient mantle massif) and substituting ρ_0 in place of ρ_m (these values differ by less than 1%) in the denominator of (8), we obtain

$$x_{oc} = H\rho_0 \beta \Delta T/(\rho_{oc} - \rho_0). \qquad (9)$$

At $H = 2.9 \times 10^6$ m, $\rho_0 = 4500$ kg/m^3, $\beta = 3 \times 10^{-5}$°C^{-1}, $\Delta T = 260$–360°C, and $\rho_{oc} = 10^4$ kg/m^3, the value of x_{oc} = 18.5–25.6 km.

For a **thermal plume,** which is produced by the melting of pure paraffin, the excess volume of molten paraffin accumulates near the plume base and solidifies, because the melting point of paraffin is lower than the temperature of the ambient thermostated water. Eventually the whole heater becomes "armored" with a shell of solidified paraffin, and, consequently, both the heater and the solidified paraffin occur to be isolated from the ambient water. As the top of the thermal plume reaches the surface of the paraffin massif ("Earth's surface"), the melt is erupted. The volume of this melt is equal to the increment in the paraffin volume owing to thermal expansion induced by the temperature increase relative to that of solid paraffin. Water cannot ascend through the conduit to a height x_w (at which hydrostatic equilibrium is established) until the paraffin shell surrounding the heater and the plume base is broken. As water ascends along the conduit, paraffin melt is erupted at the surface. The volume of this melt is equal to the volume of water in the conduit.

During the experiment, air from the molten paraffin and the surface of the heater submerged into water could accumulate near the roof of the plume. To preclude this process, the air was periodically pumped out via a capillary introduced into the plume from below. Our experimental modeling of thermochemical plume ascent demonstrates that, in the absence of an air bubble at the plume roof, the diameter of its conduits remains constant until the plume reaches the surface (Fig. 5a). In the presence of a bubble, the diameter of the plume is greater than in the previous situation and only insignificantly varies along the vertical section of the plume (Fig. 5b). Analogous phenomenon was observed during the melting of a thermal plume.

We also modeled a thermal plume that reached the boundary without melting above it. In our experiments, this was the boundary between paraffin and air or between paraffin and a metallic plate. In this situation, melting occurs along the boundary and results in a mushroom-shaped head of the plume (Fig. 6).

We also modeled a thermal plume in a two-layer system, when the plume reached a "refractory" layer whose melting point was higher than the melt temperature in the plume conduit within the lower layer. The two-layer system in our experiment was imitated by a lower layer of octadecane and an upper layer of paraffin. The melting point of octodecane is 28.2°C, i.e., is lower than the paraffin melting point by 23.8°C. When the head of the plume developing in octadecane reached the paraffin ("refractory") layer, the latter did not start melting, but instead, melting was initiated in octadecane, in the upper part of the plume and at its sidewalls. The plume acquired a mushroom morphology near the phase boundary, and the diameter of the plume head became greater than the diameter of its tail (plume conduit) (Fig. 6).

Our experimental modeling demonstrated that:

(1) the diameter of the plume remained practically constant during its ascent;

(2) a mushroom-shaped head of the plume was formed when the top of the ascending plume reached the bottom of the "refractory" layer;

(3) when the thermochemical plume reached the surface, the first melt to be erupted had a volume equal to the volume of the melt accumulated near the plume base, and the melt erupted afterward was forced out of the plume conduit by the material of the outer core.

PARAMETERS OF A THERMOCHEMICAL PLUME ASCENDING FROM THE CORE–MANTLE BOUNDARY

Based on the analysis of geological, petrological, and geophysical data and the results of our experimental modeling, we developed a model of a thermochemical plume and derived principal equations and relations for determining the parameters of a plume. In considering the heat and mass transfer of a thermochemical plume in (Kirdyashkin et al., 2004; Dobretsov et al., 2005), it was assumed that the heat flow from the outer core and thermal convection in the lower mantle induce the development of a thermal layer at the boundary between the core and mantle. The temperatures at the core–mantle boundary largely predetermine and control the origin and ascent of a plume. Moreover, this boundary is marked by chemical reactions between hydrogen and/or methane (that come to the bottom of the lower mantle from the core) and minerals. The reactions can produce chemical admixtures (fluid and eutectic mixtures and compounds) that decrease the melting temperature of material near the core–mantle boundary. The temperature decrease of mantle material, where it is doped by temperature-decreasing compounds, can bring about the origin and development of a thermochemical plume. The admixtures decreasing the melting temperatures can be transported by melts to the roof of the ascending plume via heat and mass transfer in the turbulent regime of free convection. The transport of the chemical dope to the roof decreases the melting temperature of the lower mantle material, the material melts, and the plume continues ascending.

In the problem of heat and mass transfer of a thermochemical plume, and concentrations c_1 of the chemical dope (MgO, SiO_2, H_2O, and CO) that decrease the melting temperature at the plume base are assumed to be known (Kirdyashkin et al., 2004), as also assumed to be known the temperature differences $T_{md} - T_0$ and $T_{md} - T_1$, where T_{md} is the melting temperature of the "dry" (without chemical dope) massif, T_0 is the temperature of the massif averaged over its vertical extension, and T_1 is the temperature of the plume base. The parameters to be determined include c_2, which is the concen-

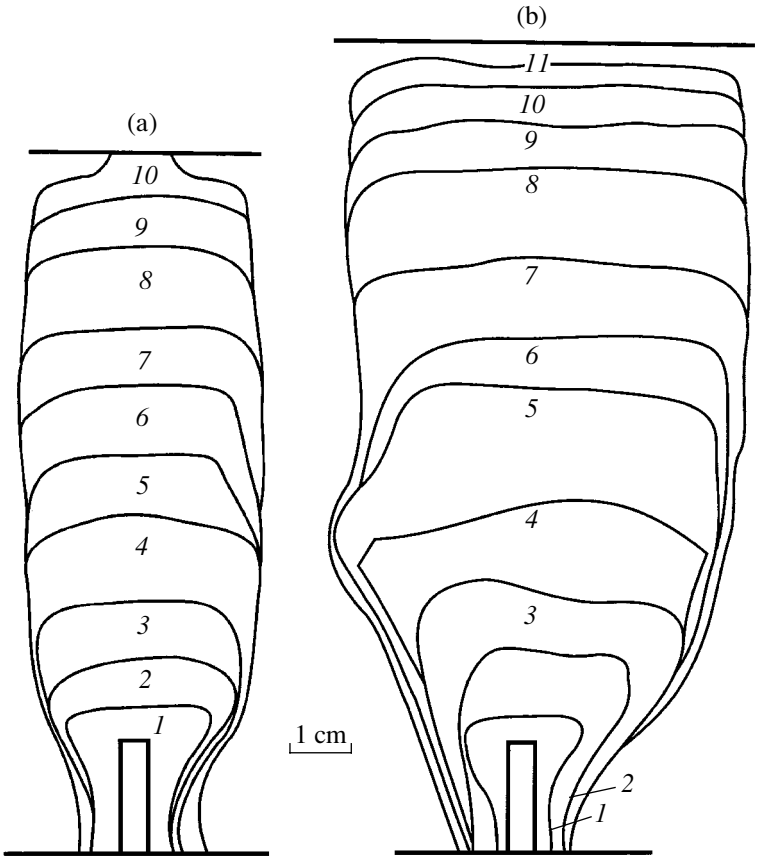

Fig. 5. Morphological evolution of a thermochemical plume whose development was triggered by doping with hexadecane (which suppresses the melting point of paraffin). (a) In the absence of air in the vicinity of the plume roof: the temperature of the ambient water $T_w = 45°C$, the thermal power of the heat source $W = 8$ W. The position of the boundary of the plume conduit varies with time t as follows: (*1*) $t = 10$ min; (*2*) $t = 15$ min; (*3*) $t = 20$ min; (*4*) $t = 35$ min; (*5*) $t = 45$ min; (*6*) $t = 56$ min; (*7*) $t = 72$ min; (*8*) $t = 97$ min; (*9*) $t = 107$ min; (*10*) $t = 117$ min. (b) In the presence of air in the vicinity of the plume roof: $T_w = 46°C$, $W = 12$ W; (*1*) $t = 10$ min; (*2*) $t = 30$ min; (*3*) $t = 45$ min; (*4*) $t = 65$ min; (*5*) $t = 80$ min; (*6*) $t = 95$ min; (*7*) $t = 110$ min; (*8*) $t = 125$ min; (*9*) $t = 140$ min; (*10*) $t = 150$ min; (*11*) 160 min.

tration of the chemical dope at the interface between the melt and ambient massif (boundaries of the plume); c_r, which is the concentration of the dope in the melt near the plume roof; T_{mc}, which is the melting temperature of the massif in the lower mantle in the presence of a chemical dope; and T_r, which is the melt temperature near the plume roof. To determine these parameters, the system of equations from (Kirdyashkin et al., 2004) should be solved. This problem was solved for $\beta = 3 \times 10^{-5}°C^{-1}$, heat conductivity coefficient $a = 10^{-6}$ m^2/s, heat conductivity of melt in the plume conduit $\lambda \approx \lambda_s = 5$ W/(m °C), average density of the ambient mantle massif $\rho = 4 \times 10^3$ kg/m^3, $B = 210$ kJ/kg, and $C = 1.2$ kJ/kg × °C (Dobretsov et al., 2005). As was demonstrated by our calculations, the most probable value of the kinematic viscosity in the plume conduit $\nu = 2$ m^2/s, the concentration of the chemical dope in the plume base $c_1 = 3\%$, and the temperature difference $T_{md} - T_0 = 420°C$ at a thermal power $N = 3.0 \times 10^8$–4.0×10^8 kW and an ascent time t = 1–5 m.y. (Kirdyashkin et al., 2004; Dobretsov et al., 2005).

Figure 7 presents the dependence of the temperature difference $T_{md} - T_1$ on the Le = a/D (where D is diffusion coefficient of the chemical dope in the plume conduit) at a thermal power of the plume equal to 3.0×10^8 to 4.0×10^8 kW and an ascent time t = 1–5 m.y. The intensity of heat and mass transfer near the plume base is controlled by the difference between the temperature at the plume base and the melting temperature of the chemically doped material $T_1 - T_{mc}$. As was mentioned above, the melting of mantle material near the core–mantle boundary is possible when the temperature difference $T_1 - T_{mc} = kc_2 - (T_{md} - T_1)$ is positive, i.e., the condition $kc_2 > T_{md} - T_1$ is satisfied. One can determine the average value of the difference $(T_{md} - T_1)$ at any Lewis number from Fig. 7. For example, at Le = 400, the average value of $(T_{md} - T_1)$ is equal to 19°C for d_s = 70 km and 36°C for d_s = 100 km. At the most probable d_s = 100 km (Sobolev, 1979; Dobretsov et al., 1980), the average value of $(T_{md} - T_1)$ increases from 22.5 to 59.5°C as the diffusion coefficient D increases from 10^{-9} to 10^{-8} m^2/s.

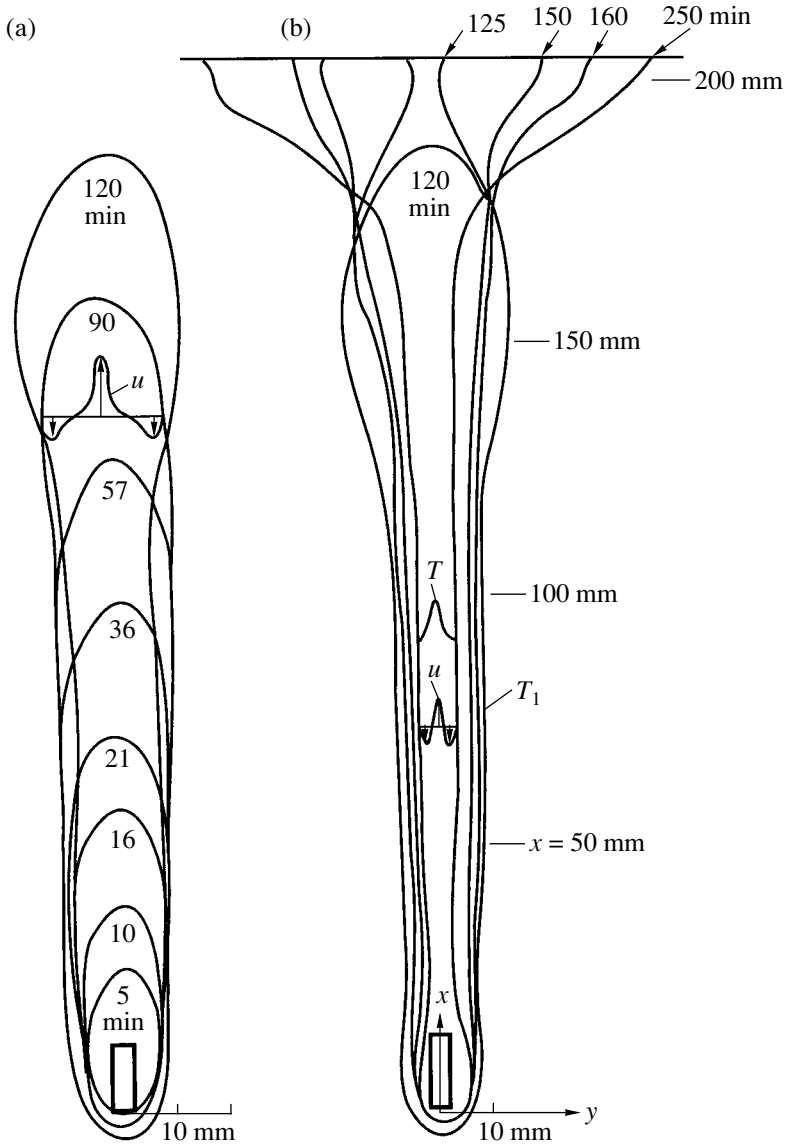

Fig. 6. Thermal plume above a local heat source during the melting in the paraffin massif.
The thermal power of the heat source $W = 9$ W, the diameter of the container is 200 mm, the temperature of the walls is 22°C. The figure demonstrates the velocities u and temperature T in the plume conduit. When the plume reaches the upper boundary, which imitates the lower boundary of a layer with a higher melting temperature, a funnel (head of the plume) is formed below this boundary. (a) Plume conduit over the time span of 0–120 min. (b) Morphology of the plume conduit over the time span of 120–250 min.

The average temperature differences $T_{md} - T_1$ determined from Fig. 7 make it possible to calculate the other parameters of a thermochemical mantle plume ascending from the core–mantle boundary (table). As follows from the table, at a temperature difference $T_1 - T_{mc} = 12$–18.5°C and a diameter $d_s = 70$–100 km, the thermal power of the plume $N = 3.5 \times 10^8$ to 4.0×10^8 kW. The possibility of the origin of a thermochemical plume at the core–mantle boundary at relatively small temperature differences $T_1 - T_{mc}$ depends on the intensity of heat transfer near the plume base. The latter is determined, at these $T_1 - T_{mc}$ values, by the low kinematic viscosity of melt in the plume conduit $\nu = 2$ m^2/s and the relatively large diameter of the plume conduit $d_s = 70$–100 km, at which the Rayleigh number (which controls the intensity of convection) $\mathrm{Ra} = \beta g \Delta T_s d_s^3 / a\nu = 3 \times 10^{17}$–$10^{18}$, where $\Delta T_s = (T_1 - T_{mc})/2$ is the temperature difference within the boundary layer near the plume base (Kirdyashkin et al., 2004; Dobretsov et al., 2005).

The results of the theoretical simulations in (Kirdyashkin et al., 2004; Dobretsov et al., 2005) and in this publication pertain to the situation when the plume conduit contains solid particles, and the fraction of melt in

the mixture is determined by the value of φ. In this situation, for a specified value of φ, the viscosity of the mixture of melt and solid particles can be determined according to experimental and theoretical data in (Persikov, 1984). The melting heat of this melt is determined as $B\varphi$, and its kinematic viscosity is $\nu = f(\varphi)$. As follows from data in (Persikov, 1984), an increase in the melt viscosity related to a decrease in the φ value from 1 to 0.7 only insignificantly affects the thermal power of the source and the time and velocity of plume ascent. Thus, the results reported in (Kirdyashkin et al., 2004; Dobretsov et al., 2005) and in this paper can be used at $0.7 \le \varphi \le 1$ without corrections for ν and B.

The intensity of the magmatic activity of plumes can be estimated as follows. According to the evaluated volumes of the magmas and the intensity of magmatism in the Phanerozoic (Dobretsov and Kirdyashkin, 1998; Larson and Olson, 1991; Kaiho and Saito, 1994), the intensity of plume-related eruptions is 2×10^6 km^3/m.y. over the past 50 m.y, i.e., $\Delta V_f = 63.7$ m^3/s, and, at $\rho_f = 2700$ kg/m^3, the mass flux $\Delta G = \rho_f \Delta V_f = 1.72 \times 10^5$ kg/s. For $C = 1.2$ kJ/kg °C, $\beta = 3 \times 10^{-5}$°C^{-1}, and the deduced value of ΔG, the overall thermal power of plumes is, according to (5), $\Sigma N = 6.88 \times 10^{12}$ W = 6.88×10^9 kW, which equals 19% of the thermal power arriving from the Earth's interiors to its surface.

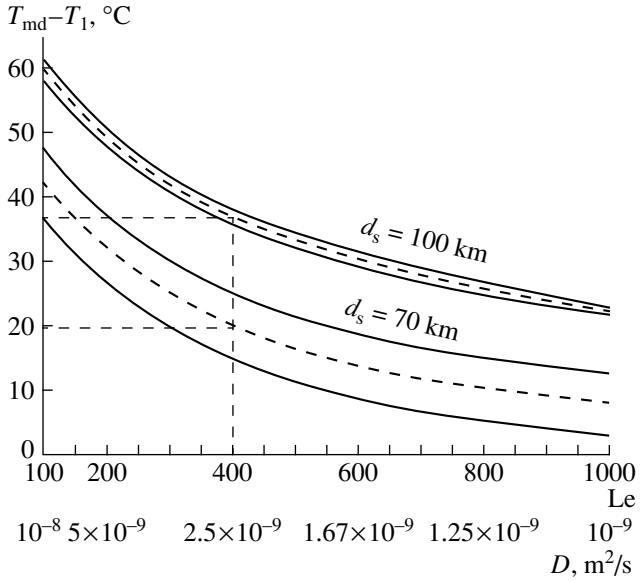

Fig. 7. Dependence of the temperature difference $T_{md} - T_1$ on the Lewis number Le (diffusion coefficient D) at a thermal power of the plume $N = (3.0–4.2) \times 10^8$ kW, ascent time of the plume t = 1–5 m.y, c_1 = 3%, ν = 2 m^2/s, $T_{md} - T_0$ = 420°C, and d_s = 70 and 100 km. Dashed lines show the average values of the temperature difference $T_{md} - T_1$ for corresponding diameters d_s.

CONDITIONS UNDER WHICH AN ERUPTION CONDUIT IS FORMED

Kirdyashkin et al. (2005) considered the geodynamic processes occurring during the derivation of a plume and its ascent to the surface. Figures 8 and 11 present a scheme of the rise of a plume to the Earth's surface. When the diameter of the plume roof d_r is greater than or equal to the diameter of the conduit d_1 ($d_r \ge d_1$), the pressure in the melt beneath the roof of the plume is higher than the lithostatic pressure above the plume roof by a value of ΔP

$$\Delta P = \rho_0 g x_1 \beta (T_m - T_0)(d_1/d_r)^2, \qquad (10)$$

where ρ_0 is the density of the ambient solid lithospheric massif, g is the gravitational acceleration, x_1 is the height of the plume, β is the coefficient of thermal volumetric expansion of melt in the plume conduit, T_m is the temperature of the melt, and T_0 is the temperature of the ambient massif. The pressure on the roof of the plume ΔP induces the displacement and deformation of the overlying rock layers. The rheology of the layer above the plume roof is complicated: the lower (lithospheric) part of this layer can be represented in the form of a viscous medium, whereas the upper crustal layer is a viscoelastic or elastic medium. If the thickness of the layer immediately overlying the plume roof is much greater than the thickness of the crustal layer, the motions above the roof of an ascending plume can be visualized as movements in a viscous liquid in front of a moving roof (Schlichting, 1969). As a simplifying approximation, motions in the massif above the roof of an ascending plume of diameter d_r can be regarded as a viscous flow in a cylindrical conduit of diameter d_r and height $H - x_1$ (in Fig. 8 the conduit is shown with dashed lines).

Theoretical modeling demonstrates that, during the ascent of a plume d_r in diameter, the roof reaches a critical height x_{2cr} at which the shear stress in the massif above the plume roof reaches a limiting value τ_{cr}, and one or more conduits can develop in the vicinity of the cylindrical surface of the massif above the plume roof of diameter d_r. These conduits can be used by the mag-

Parameters of a thermochemical plume ascending from the core–mantle boundary at average values of $T_{md} - T_1$ (Fig. 7) corresponding to Lewis numbers within the range of Le = 100–1000, d_s = 70 and 100 km, $T_{md} - T_0$ = 420°C, c_1 = 3%, and ν = 2 m^2/s

d_s, km	c_2, %	c_r, %	$T_1 - T_{mc}$, °C	$T_r - T_{mc}$, °C	$T_{mc} - T_0$, °C	N, kW	t, m.y.	$\bar{u}$, m/year
70	1.1	2.1	18.5	9.8	381	3.5×10^8	2.7	1.1
100	1.4	2.2	12	6	371	4.0×10^8	4.8	0.6

Note: $\bar{u}$ is the average velocity of plume ascent. See text for symbol explanations.

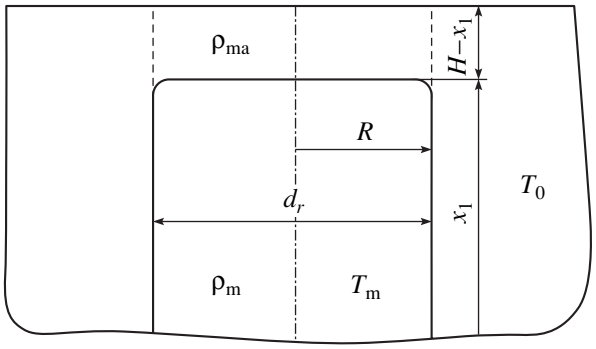

Fig. 8. Scheme of the ascent of a mantle plume when it approaches the surface and the plume conduit diameter is equal to the roof diameter d_r. H is the maximum height of plume ascent from the core–mantle boundary. See text for explanations.

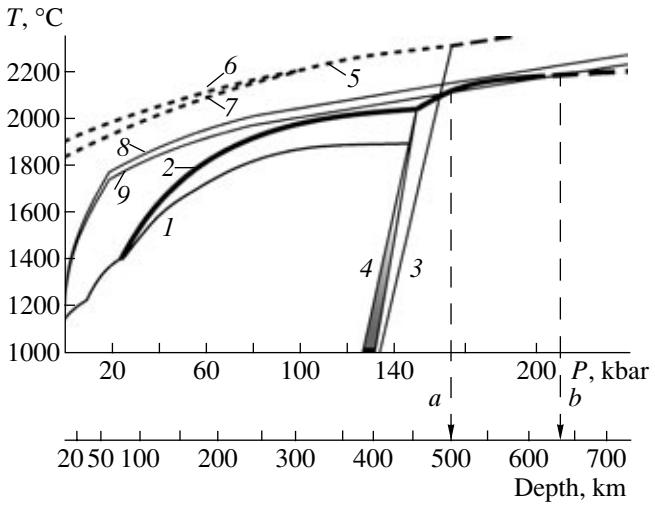

Fig. 9. Melting temperature of natural peridotite and changes in temperature in the melt near the roof of an ascending plume (for the upper mantle). (*1*) Melting temperature of natural peridotite KLB-1 (Takahashi, 1986); (*2*) melting temperature of natural peridotite KLB-1 (Herzberg and Zhang, 1996); (*3*) transition of forsterite to modified spinel (Presnall et al., 1998); (*4*) field of the olivine–ringwoodite transition (Herzberg and Zhang, 1996); lines *5*–*7* are after (Presnall et al., 1998); (*5*) incongruent melting of forsterite with the origin of periclase and liquid under pressures of >100 kbar; (*6*) incongruent melting of forsterite under pressures of <100 kbar; (*7*) forsterite + periclase = liquid eutectic; (*8*) variations in the melt temperature near the roof of an ascending plume in the absence of intersection with the melting line of peridotite KLB-1; (*9*) variations in the melt temperature near the roof of a plume with depth at intersection with the melting line of peridotite KLB-1. The pressure–depth relations are shown according to (Zharkov, 1983).

matic melt for eruptions at the surface. The value x_{2cr} is the height of these eruption conduits or, in other words, the depth from which the magma ascends to the surface along the eruption conduit.

For plumes ascending from the core–mantle boundary and whose roofs and conduits have equal diameters, the value of x_{2cr} lies within the range of 44 to 92 km at the diameter of the plume equal to 40–100 km (Kirdyashkin et al., 2005). These results are consistent with the depth values evaluated from the *P–T* estimates for mantle xenoliths in basanites from various areas in the United States and Australia, alkali basalts in central Mongolia, southern Transbaikalia, and the Vitim volcanic field (Dobretsov, 1980; Zonenshain and Kuz'min, 1983; Ashchepkov, 1991; Dobretsov and Ashchepkov, 1991; Ionov et al., 1993a, 1993b; Ashchepkov et al., 1996; Litasov et al., 2000; Irving, 1980; Stosh et al., 1995; Kopylova et al., 1995).

DEPENDENCE OF THE MORPHOLOGY AND SIZE OF A PLUME ROOF ON THE *P–T* CONDITIONS

According to the results of our experiments, at a constant melting temperature of the massif, the diameter of the melted plume conduit does not vary in the vertical section. Theoretical considerations indicate that, at a constant diameter of a plume ($d_r/d_1 = 1$), it breaks through to the surface from depths of 44–92 km. These calculated results are consistent with data on mantle xenoliths in alkali basalts. Considering the change in the melt density due to the physicochemical transformations in response to melt chemical doping, the pressure difference ΔP should be greater than the value postulated by (6), which was derived with regard for the thermal expansion alone. Then the depth from which a plume ascends should be greater and the obtained values. Our results indicate that, at a constant melting temperature of the ambient massif, the diameter of the plume conduit practically does not vary with depth, and the diameter of the plume roof is comparable with the diameter of the conduit of the plume.

Model experiments reveal an increase in the diameter of a plume roof compared with the diameter of its conduit when the roof of the plume reaches a "refractory" layer, whose melting temperature is higher than the melting temperature of the underlying layer and the temperature in the plume conduit. In this situation, melting occurs in the underlying layer, along the boundary of the layers, and a mushroom-shaped plume head is formed (Fig. 6). This situation can arise at (i) a certain relations between the melting temperature of the massif and the temperature of the melt near the roof of the plume during its ascent; and (ii) near the bottom of the lithosphere, if the lithospheric part of the mantle is dominated by dunites and harzburgites (Kirdyashkin et al., 2005).

Figure 9 demonstrates melting lines *1* and *2* for peridotite KLB-1 from (Takahashi, 1986; Herzberg and Zhang, 1996). The positions of the melting lines are somewhat different, and their divergence increases with pressure and reaches almost 150°C at a pressure of 140 kbar. The analysis of details of the experimental

techniques utilized by these researchers did not allow us to reveal the reasons for the differences between the lines and did not provide us with any grounds for giving preference to any of them. However, considering that the data from (Herzberg and Zhang, 1996) cover a broader range of conditions, including pressures above the olivine–ringwoodite transition, these data seem to be more suitable for our analysis of plume behavior. The configurations of the melting lines for peridotite KLB-1 are similar and resemble most melting lines under high pressures, both for eutectic and individual minerals. For example, Fig. 9 shows lines *5–7* of the monovariant melting reactions of forsterite, whose dT/dP derivatives vary in a similar manner.

Figure 9 also displays the variations in the melt temperature near the plume roof according to the adiabatic law, with an adiabatic gradient $(\partial T/\partial x)_{ad} = 0.56$°C/km (lines *8* and *9*). This approximation is valid at the depths in question. The temperature variations in compliance with line *8* are typical of plumes with a relatively low heat flux from the plume conduit to the ambient lower mantle massif (Hawaii and Iceland). Line *8* passes above line *2*, i.e., the temperature of the melt near the plume roof is always higher than the melting temperature of the ambient massif. In this situation, the diameter of the conduit remains unchanging throughout its whole vertical extent, and the plume breaks through to the surface as is shown for $d_r/d_1 = 1$.

Now consider the situation when the temperature of the melt near the roof of the plume varies according to law *9* (Fig. 9). This situation can be characteristic of plumes with a more significant heat flux from their conduits to the ambient lower mantle massifs due to horizontal convection flows in the lower mantle. Line *9* intersects line *2* at points *a* and *b* and, hence, the upper mantle should contain layer *a–b* (with roof *a* and bottom *b*) whose melting temperature is higher than the melt temperature near the plume roof. This layer was referred to above as the "refractory" layer. Judging from the position of line *9* (Fig. 9), the bottom *b* of this layer is situated at a depth of 645 km, and its roof *a* is at a depth of 500 km, which is close to the geophysical parameters of transition layer *C* in the upper mantle (Zharkov, 1983; Zhao, 2001). Melting occurs at boundary *b* and results in a mushroom-shaped head of the plume. The only driving force of the further ascent of the plume above boundary *b* (within layer *a–b*) is the buoyancy force, i.e., a plume can ascent through "refractory" layer *a–b* due to the difference between the densities of the plume and the ambient layer.

To the left of intersection point *a*, line *9* passes above melting line *2* (Fig. 9), which means that, as soon as the roof of the plume reaches the upper boundary *a* of the "refractory" layer, the melting and ascent of the plume are resumed, i.e., plume again ascents above boundary *a* in compliance with the thermochemical mechanism and eventually breaks to the surface, as was described above for a constant diameter of the plume conduit.

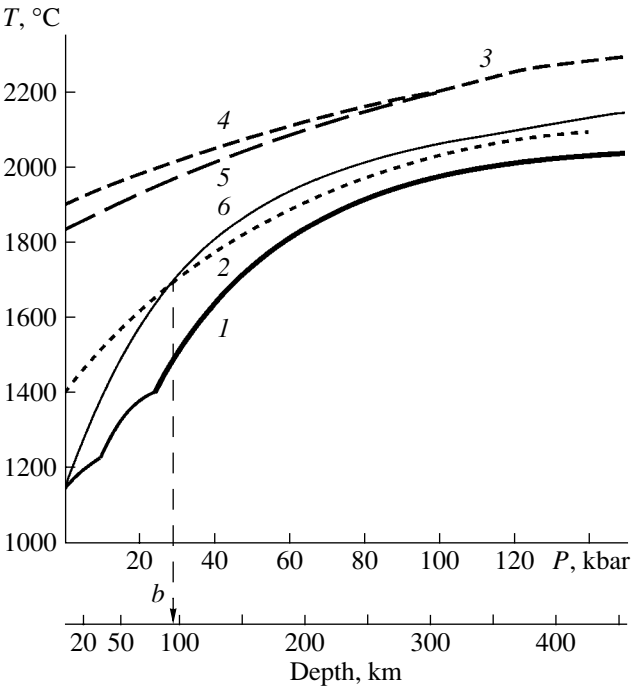

Fig. 10. Dependence of the melting temperature of natural peridotite and the melt temperature near the roof of an ascending plume on depth (pressure). (*1*) Melting temperature of natural peridotite KLB-1 (Herzberg and Zhang, 1996); (*2*) probable melting line of rocks in the depleted mantle, when the olivine content in the peridotite is 30% higher than that in peridotite KLB-1; (*3*, *4*, *5*) melting lines of pure forsterite according to the reactions forsterite = periclase + liquid, forsterite = liquid, and forsterite + periclase = liquid, respectively (Presnall et al., 1998); (*6*) variations in the melt temperature near the roof of an ascending plume. The pressure–depth relations are shown according to (Zharkov, 1983).

A "refractory" layer can also be formed at the bottom of the lithosphere. The profound differentiation of the material results in the depletion of the mantle in low-melting components and its enrichment in the refractory olivine-bearing component (Dobretsov, 1980; Dobretsov and Kirdyashkin, 1998). These conditions are favorable for the origin of a layer composed of rocks of the harzburgite–dunite type. Line *2* in Fig. 10 corresponds to the probable melting of rocks in the depleted mantle, when the mantle peridotite contains 30% more olivine than peridotite KLB-1. Line *6* in the same figure demonstrates the melt temperature near the roof of an ascending plume. This configuration of the melting line is made possible by the intense heat transfer from the plume conduit to the asthenosphere. No melting of overlying rocks is possible above boundary *b*, because line *2* lies in this region above line *6*. Thus, the melting zone expands along boundary *b* and produces a mushroom-shaped head of the plume. The further ascent of the plume is possible if the density of the

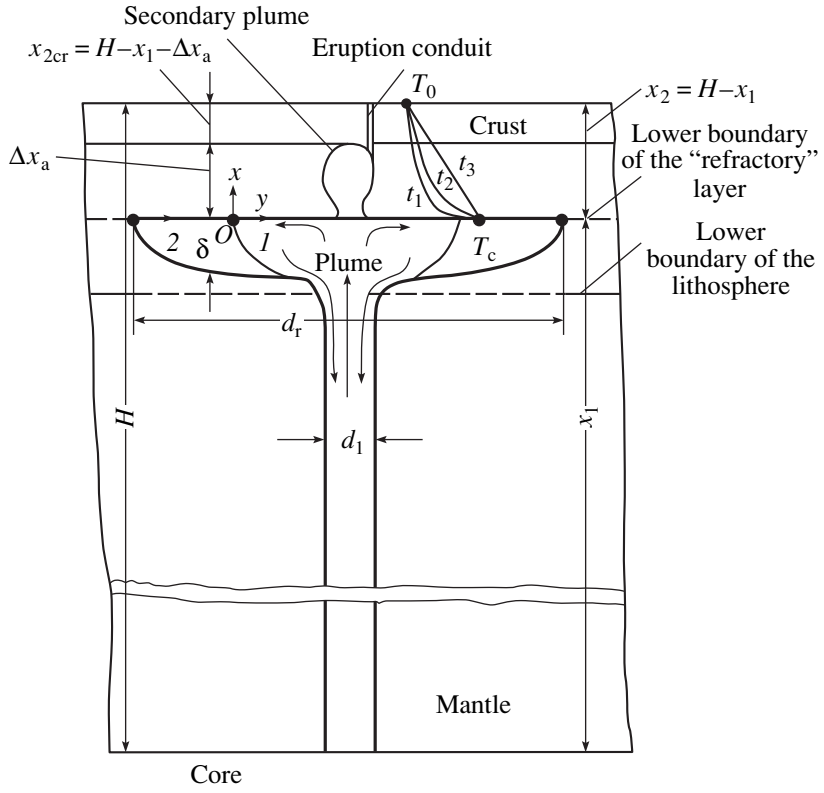

Fig. 11. Schematic representation of the evolution of the head of a plume that reached the lower boundary of a "refractory" layer. δ is the thickness of the plume head, $x_2 = H - x_1$ is the depth of the lower boundary of the "refractory" layer, Δx_a is the height to which the secondary plume can ascend, $x_{2cr} = H - x_1 - \Delta x_a$ is the height of the eruption conduit. The temperature profiles across the "refractory" layer x_2 are presented for moments of time $t_1 < t_2 < t_3$, respectively. *1* and *2* are the positions of the plume head at t_1 and t_2, respectively. Free convective flows in the plume are shown.

melt in the plume conduit is lower than the density of the overlying rocks, and the pressure at the plume roof is higher than the lithostatic pressure.

If the diameter of the plume head is much greater than the diameter of the plume conduit and the thickness of the plume head, a number of secondary plumes can be formed. They ascend through the "refractory" layer because of the difference between the densities of the material in the plume conduit and that of the ambient lithospheric massif. Upon reaching a critical depth x_{2cr}, the secondary plume breaks through the overlying rocks and erupts at the surface. The situations of a "refractory" layer considered above seem to pertain to flood-basalt eruptions of great volume, such as the Siberian traps (Dobretsov, 1997; Dobretsov et al., 2001).

DIAMETER OF THE PLUME HEAD AND THE TIME OF ITS FORMATION AT THE BOTTOM OF THE "REFRACTORY" LITHOSPHERIC LAYER

Upon reaching the bottom of the "refractory" lithospheric layer, whose temperature is higher than the temperature of material in the plume conduit, the plume spreads along the lower boundary of this layer and forms a mushroom-shaped head (Figs. 6, 11). The plume further breaks to the surface in the following manner. A purely chemical secondary plume develops at the lower boundary of the "refractory" layer (the boundary between the plume and the "refractory" layer) due to the difference between the densities of the plume melt and the rocks above the plume roof (Fig. 11). The secondary plume ascends through the "refractory" layer, from its lower boundary to a height Δx_a from which the plume can break through the overlying rocks to the surface and erupt.

The diameter of the plume head near the lower boundary of the "refractory" layer was determined as depending on the thermal power of the plume source and time t (Dobretsov et al., 2006) based on the balance of heat flows within the plume head (the heat transferred by the plume over time t to the ambient lithospheric massif and spent on the heating of the ambient massif and its melting).

As a simplifying approximation, we regard the secondary plume as spherical and assume that it ascends through the "refractory" layer in compliance with the Stokes formula for the movement of a sphere through a highly viscous liquid (Schlichting, 1969). Within the

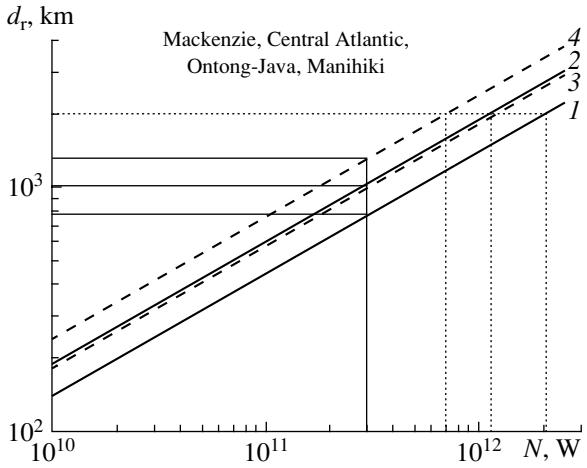

Fig. 12. Dependence of the plume head diameter on the thermal power of the plume at d_1 = 100 km and degree of melting φ = 0.3. (*1*) x_2 = 100 km, Δx_a = 70 km, η = 5×10^{21} (N s)/m^2, t = 2.9 m.y.; (*2*) x_2 = 200 km, Δx_a = 170 km, η = 5×10^{21} (N s)/m^2, t = 7.1 m.y.; (*3*) x_2 = 100 km, Δx_a = 70 km, η = 10^{22} (N s)/m^2, t = 5.8 m.y. (*4*) x_2 = 200 km, Δx_a = 170 km, η = 10^{22} (N s)/m^2, t = 14.2 m.y.

scope of this approximation, we have determined the ascent velocity and time of a secondary plume. The head of the plume stops growing when the secondary plume reaches the surface. Thus, the growth time of the mushroom-shaped head of the main (thermochemical) plume is commensurable with the ascent time of the secondary (chemical) plume through the "refractory" layer. The ascent time of the secondary plume within the "refractory" layer t = 3–14 m.y. (Dobretsov et al., 2006), depending on the dynamic viscosity η and the depth of the "refractory" layer.

At a thermal power of a plume $N = 3 \times 10^{11}$ W and viscosity of the "refractory" lithospheric layer η = 5×10^{21}–10^{22} (N s)/m^2, the diameter of the plume head d_r at which the plume erupts can be 770–1310 km (Fig. 12). The average growth rate of a plume head depends on the power of the plume source, the diameter of its head, and the ascent time of the secondary plume through the "refractory" layer. At $N = 3 \times 10^{11}$ W, d_r = 770–1310 km, and t = 3–14 m.y., the average growth rate of a plume head $u_r = d_r/t$ can range between 10 and 25 cm/year.

According to the estimates in (Ernst and Buchan, 2002; Ernst et al., 2005), the diameter of a plume head for such greatest continental flood-basalt provinces as Mackenzie and Central Atlantic and the oceanic plateaus Ontong–Java and Manihiki $d_r \approx 2000$ km. The Siberian traps are of the same order (Dobretsov et al., 2001). As can be seen from Fig. 12, the thermal power of a plume source at such a diameter can vary from 7×10^{11} to 2×10^{12} W.

CONCLUSIONS

In conclusion, it should be mentioned that our results are close to the earlier semiempirical estimates of some plume parameters obtained by W.J. Morgan (Morgan, 1971; quoted from Holden and Vogt, 1977). Morgan has estimated the ascent velocity of plumes through the mantle at 2 m/year (our estimates are 0.5–2 m/year), the ascent time of a plume at 1.5 m.y. (our estimates are 1–5 m.y.), with the diameter of the mushroom-shaped head of a plume also consistent with our maximum estimates. As could be expected, the geological consequences are also similar, and the estimates are confirmed by geological evidence. At the same time, our modeling of thermochemical plumes differs from experiments in which the ascent of a plume is modeled by a low-viscous material ascending through a highly viscous medium (Campbell and Griffiths, 1990; Griffiths and Campbell, 1991).

Our results are underlain by geological and geophysical materials, our original and literature data, physical experiments approximating naturally existing thermochemical plumes, and theoretical modeling. We hope that these results provide better insight into both geodynamic processes related to mantle plumes and their geological consequences.

In this publication, we did not touch upon a wide circle of problems related to mineralogical and geochemical lines of evidence for the lower mantle origin and evolution of plumes. Inasmuch as plumes not only are produced in the mantle of variable composition but also exchange volatile components with it, the material in the axial zones of plume-related eruptions (such as Hawaii) contains much of the lower mantle component: from 90% (according to isotopic–geochemical evidence based on He, Os, and Sr isotopic ratios) to 25–40% (according to mineral- and whole-rock geochemical data with regard for such parameters as the Ca and Ni ratios in olivine and thermobarometric data) (see, for example, Walker et al., 1995; Brandon et al., 1998, 1999, 2003; Sobolev et al., 2005). The content of the lower mantle component in the marginal portions of plumes and the products of their differentiation can decrease to zero.

These problems deserve separate consideration, but in any event, the mineralogical and geochemical features and, particularly, isotopic–geochemical data provide extremely important information that can be used to refine and further detail the theory of mantle plumes. A significant role belongs here to seismographic and other data of deep geophysics. Recently obtained seismic tomographic materials (for example, in Zhao, 2001, 2004) are generally consistent with our results and also suggest that mantle plumes are systematically curved, and their thermal aureoles expand under the effect of mantle convective flows.

Finally, the theory of lower mantle and two-storey plumes should be naturally compatible with plate tectonics, whose driving forces are convective flows in the

mantle. Zonenshain and Kuz'min (1983, 1993) and the authors of this paper (Dobretsov and Kirdyashkin, 1994, 1998; Dobretsov et al., 2001) published evidence in support of the two-storey tectonic structure and evolution of the Earth: the tectonics of lithospheric plates and hot fields.

ACKNOWLEDGMENTS

This study was financially supported by the Russian Foundation for Basic Research (project no. 05-05-64899a), a grant for leading research schools from the President of the Russian Federation (Grant NSH-8872.2006.5), a grant for the support of junior researchers of Russia (candidates of science and their scientific supervisors) from the President of the Russian Federation (Grant MK-2496.2006.5), and a grand from the Siberian Division of the Russian Academy of Sciences (interdisciplinary integration project no. 52 "Modeling of Mantle Thermochemical Plumes in Various Geodynamic Settings).

REFERENCES

1. I. V. Ashchepkov, *Deep-Seated Xenoliths of the Baikal Rift* (Nauka, Novosibirsk, 1991) [in Russian].
2. I. V. Ashchepkov, Yu. D. Litasov, and K. D. Litasov, "Garnet Peridotite Xenoliths from Melanephelinites of the Hentey Ridge, Southern Transbaikalia: Evidence for a Rising Mantle Diapir," Geol. Geofiz. **37** (1), 130–147 (1996).
3. A. D. Brandon, M. D. Norman, R. J. Walker, and J. W. Morgan, "^{186}Os–^{187}Os Systematics of Hawaiian Picrites," Earth Planet. Sci. Lett. **174**, 25–42 (1999).
4. A. D. Brandon, R. J. Walker, I. S. Puchtel, et al., "^{186}Os–^{187}Os Systematics of Gorgona Island Komatiites: Implications for Early Growth of the Inner Core," Earth Planet. Sci. Lett. **206**, 411–426 (2003).
5. A. D. Brandon, R. J. Walker, J. W. Morgan, et al., "Coupled ^{186}Os and ^{187}Os Evidence for Core–Mantle Interaction," Science **280**, 1570–1573 (1998).
6. I. H. Campbell and R. W. Griffiths, "Implications of Mantle Plume Structure for the Evolution of Flood Basalts," Earth Planet. Sci. Lett. **99**, 79–83 (1990).
7. N. L. Dobretsov and A. G. Kirdyashkin, "Sources of Mantle Plumes," Dokl. Akad. Nauk **373** (1), 84–86 (2000) [Dokl. Earth Sci. **373**, 879–881 (2000)].
8. N. L. Dobretsov and A. G. Kirdyashkin, "Estimation of Global Exchange Processes between Earth's Shells: Comparison of Geological Observations and Theoretical Data," Geol. Geofiz. **39** (9), 1269–1279 (1998).
9. N. L. Dobretsov and A. G. Kirdyashkin, *Deep-Level Geodynamics* (Brookfield: Balkema, Rotterdam, 1998).
10. N. L. Dobretsov and A. G. Kirdyashkin, *Deep-Level Geodynamics* (SO RAN, NITs OIGGM SO RAN, Novosibirsk, 1994) [in Russian].
11. N. L. Dobretsov and I. V. Ashchepkov, "Evolution of the Upper Mantle beneath the Baikal Rift Zone," Geol. Geofiz., No. 1, 3–16 (1991).
12. N. L. Dobretsov, "Permian–Triassic Magmatism and Sedimentation in Eurasia as a Result of a Superplume," Dokl. Akad. Nauk **354**, 220–223 (1997) [Dokl. Earth Sci. **354**, 497–500 (1997)].
13. N. L. Dobretsov, *Introduction in Global Petrology* (Nauka, Novosibirsk, 1980) [in Russian].
14. N. L. Dobretsov, A. A. Kirdyashkin, and A. G. Kirdyashkin, "Diameter and Formation Time of Plume Head at the Base of Refractory Lithospheric Layer," Dokl. Akad. Nauk **406**, 99–103 (2006) [Dokl. Earth Sci. **406**, 56–60 (2006)].
15. N. L. Dobretsov, A. A. Kirdyashkin, and A. G. Kirdyashkin, "Physicochemical Conditions at the Core–Mantle Boundary and Formation of Thermochemical Plumes," Dokl. Akad. Nauk **393**, 797–801 (2003) [Dokl. Earth Sci. **393**, 1319–1322 (2003)].
16. N. L. Dobretsov, A. G. Kirdyashkin, and A. A. Kirdyashkin, "Parameters of Hot Spots and Thermochemical Plumes," Geol. Geofiz. **46**, 589–602 (2005).
17. N. L. Dobretsov, A. G. Kirdyashkin, and A. A. Kirdyashkin, *Deep-Level Geodynamics* (SO RAN, GEO, Novosibirsk, 2001) [in Russian].
18. N. L. Dobretsov, A. G. Kirdyashkin, and I. N. Gladkov, "Problems of Deep-Level Geodynamics and Modeling of Mantle Plumes," Geol. Geofiz. **34** (12), 5–21 (1993).
19. *Experimental Problems of Geology*, Ed. by V. A. Zharikov and V. V. Fed'kin (Nauka, Moscow, 1994) [in Russian].
20. R. E. Ernst and K. L. Buchan, "Maximum Size and Distribution in Time and Space of Mantle Plumes: Evidence from Large Igneous Provinces," J. Geodynam. **34**, 309–342 (2002).
21. R. E. Ernst, K. L. Buchan, and I. H. Campbell, "Frontiers in Large Igneous Province Research," Lithos **79**, 271–297 (2005).
22. R. W. Griffiths and I. H. Campbell, "Interaction of Mantle Plume Heads with the Earth's Surface and Onset of Small-Scale Convection," J. Geophys. Res. **96** (B11), 18295–18310 (1991).
23. C. Herzberg and J. Zhang, "Melting Experiments on Anhydrous Peridotite KLB-1: Compositions of Magmas in the Upper Mantle and Transition Zone," J. Geophys. Res. **101** (B4), 8271–8295 (1996).
24. J. C. Holden and P. R. Vogt, "Graphic Solutions to Problems of Plumacy," EOS, Trans. Amer. Geophys. Union **58**, 573–580 (1977).
25. D. A. Ionov, I. V. Aschepkov, H.-G. Stosch, et al., "Garnet Peridotite Xenoliths from the Vitim Volcanic Field, Baikal Region: The Nature of the Garnet–Spinel Peridotite Transition Zone in the Continental Mantle," J. Petrol. **34**, 1141–1175 (1993a).
26. D. A. Ionov, I. V. Ashchepkov, H. G. Stosch, et al., "Garnet Peridotite Xenoliths of the Vitim Volcanic Field, Trans-Baikal Region: Petrology and Geochemistry of Garnet–Spinel Peridotites of Transitional Zone of Subcontinental Mantle," in *Magmatism of Rifts and Fold Belts*, Ed. by O. A. Bogatikov, H. A. Seck, V. A. Kononova, and H. J. Lippolt (Nauka, Moscow, 1993b) [in Russian].
27. A. J. Irving, "Petrology and Geochemistry of Composite Ultramafic Xenoliths in Alkalic Basalts and Implications

for Magmatic Processes within the Mantle," Am. J. Sci. **280A**, 389–426 (1980).

28. G. Ito and J. Lin, "Oceanic Spreading Center–Hotspot Interactions: Constraints from Along-Isochron Bathymetric and Gravity Anomalies," Geology **23**, 657–660 (1995).
29. K. Kaiho and S. Saito, "Oceanic Crust Productions and Climate Change During the Last 100 Ma," Terra Nova **6**, 376–384 (1994).
30. V. E. Khain, *Main Problems of Modern Geology* (Nauka, Moscow, 1995) [in Russian].
31. A. G. Kirdyashkin and I. N. Gladkov, "Thermal Plumes and Hot Spot of the Earth," Dokl. Akad. Nauk **339** (2), 250–252 (1994).
32. A. A. Kirdyashkin, N. L. Dobretsov, A. G. Kirdyashkin, et al., "Hydrodynamic Processes Associated with Plume Ascent and Conditions for Eruption Conduit Formation," Geol. Geofiz. **46**, 891–907 (2005).
33. A. A. Kirdyashkin, N. L. Dobretsov, and A. G. Kirdyashkin, "Thermochemical Plumes," Geol. Geofiz. **45** (9), 1057–1073 (2004).
34. M. G. Kopylova, S. Y. O'Reilly, and Yu. S. Genshaft, "Thermal State of the Lithosphere Beneath Central Mongolia: Evidence from Deep-Seated Xenoliths from the Shavaryn–Tsaram Volcanic Centre in the Tariat Depression, Hangai, Mongolia," Lithos **36**, 227–242 (1995).
35. R. L. Larson and P. Olson, "Mantle Plumes Control Magnetic Reversal Frequency," Earth Planet. Sci. Lett. **107**, 437–447 (1991).
36. K. D. Litasov, Yu. D. Litasov, A. S. Mekhonoshin, and V. T. Mal'kovets, "Geochemistry of Clinopyroxenes and Petrogenesis of Mantle Xenoliths from Pliocene Basanites of the Dzhilinda River, Vitim Volcanic Field," Geol. Geofiz. **41**, 1534–1556 (2000).
37. M. Manga and R. Jeanloz, "Implications of a Metal-Bearing Chemical Boundary Layer in D" for Mantle Dynamics," Geophys. Res. Lett. **23**, 3091–3094 (1996).
38. W. J. Morgan, "Convection Plumes in the Lower Mantle," Nature **230**, 42–43 (1971).
39. E. S. Persikov, *Viscosity of Magmatic Melts* (Nauka, Moscow, 1984) [in Russian].
40. D. C. Presnall, Y.-H. Weng, C. S. Milholland, and M. J. Walter, "Liquidus Phase Relations in the System $MgO–MgSiO_3$ at Pressures up to 25 GPa—Constraints on Crystallization of a Molten Hadean Mantle," Phys. Earth. Planet. Inter. **107**, 83–95 (1998).
41. P. A. Rona, "Hydrothermal Mineralization at Seafloor Spreading Centers," Earth Sci. Rev. **20**, 1–104 (1984).
42. S. Saxena, "Thermodynamics of Iron at Core Physical Conditions and Chemistry of the Core," in *Role of the Superplumes in the Earth System from Central Core to Surface Including Evolution of Life* (Japan, Tokyo, 2002), pp. 194–195.
43. C. K. Seyfert, "Mantle Plumes and Hotspots," in *Encyclopedia of Structural Geology and Plate Tectonics*, Ed. by C. K. Seyfert (Van Nostrand Reinhold, New York, 1987; Mir, Moscow, 1991), pp. 19–38.
44. H. Schlichting, *Boundary Layer Theory* (McGraw-Hill, New York, 1968; Nauka, Moscow, 1969).
45. S. V. Sobolev, "Gravitational Effect and Evolution of Low-Viscosity Channels in Mantle," Dokl. Akad. Nauk SSSR **246**, 1070–1074 (1979).
46. A. V. Sobolev, A. W. Hofmann, S. V. Sobolev, and I. K. Nikogosian, "An Olivine-free Mantle Source of Hawaiian Shield Basalts," Nature **434**, 590–597 (2005).
47. H.-G. Stosch, D. A. Ionov, I. S. Puchtel, et al., "Lower Crustal Xenoliths from Mongolia and Their Bearing on the Nature of the Deep Crust Beneath Central Asia," Lithos **36** (3–4), 227–242 (1995).
48. P. J. Tackley, "The Observational Signature of Deep Mantle Chemical Layering: Are Superplumes Thermochemical," in *Role of the Superplumes in the Earth System from Central Core to Surface Including Evolution of Life. Abstracts* (Japan, Tokyo, 2002), pp. 398–402.
49. E. Takahashi, "Melting of a Dry Peridotite KLB-1 up to 14 GPa: Implications on the Origin of Peridotitic Upper Mantle," J. Geophys. Res. **91** (B9), 9367–9382 (1986).
50. P. R. Vogt, "Global Magmatic Episodes: New Evidence and Implications for the Steady-State Mid-Oceanic Ridge," Geology **7** (2), 93–98 (1979).
51. P. R. Vogt, "Plumes, Subaxial Pipe Flow, and Topography Along the Mid-Oceanic Ridge," Earth Planet. Sci. Lett. **29**, 309–325 (1976).
52. R. J. Walker, J. W. Morgan, and M. F. Horan, "Osmium-187 Enrichments in Some Plumes: Evidence from Core–Mantle Interaction," Science **269**, 819–822 (1995).
53. D.-P. Zhao, "Global Tomographic Images of Mantle Plumes and Subducting Slabs: Insight Into Deep Earth Dynamics," Phys. Earth Planet. Inter. **146**, 3–34 (2004).
54. D.-P. Zhao, "Seismic Structure and Origin of Hotspots and Mantle Plumes," Earth Planet. Sci. Lett. **192**, 251–265 (2001).
55. V. A. Zharikov, *Principles of Physicochemical Petrology* (Mosk. Gos. Univ., Moscow, 1976) [in Russian].
56. V. N. Zharkov, *Internal Structure of the Earth and Planets* (Nauka, Moscow, 1983) [in Russian].
57. L. P. Zonenshain and M. I. Kuz'min, "Deep-Level Geodynamics of the Earth," Geol. Geofiz. **34** (4), 3–13 (1993).
58. L. P. Zonenshain and M. I. Kuz'min, "Within-Plate magmatism and Its Significance for Understanding Processes in the Earth's Mantle," Geotektonika, No. 1, 28–45 (1983).